

Neutronics modeling of the CROCUS reactor with SERPENT and PARCS codes

Adolfo Rais¹, Daniel Siefman¹, Mathieu Hursin², Andrew Ward³, Andreas Pautz^{1,2}

¹Laboratory for Reactor Physics and Systems Behaviour, École polytechnique fédérale de Lausanne, Lausanne, Switzerland

²Laboratory for Reactor Physics and Systems Behaviour, Paul Scherrer Institut, Villigen, Switzerland

³Department of Nuclear Engineering and Radiological Sciences, University of Michigan, Ann Arbor, United States

Abstract - This paper reports the methodology used for the neutronic modelling of the CROCUS reactor and discusses the challenges encountered during the process. Full-core steady-state neutronics solutions were computed with the PARCS code. The Serpent Monte Carlo code was used for few-group constant generation. The full-core Serpent model of the reactor was also used as reference for the comparison against PARCS results. The comparison between Serpent and PARCS solutions was successful, achieving good level of agreement for eigenvalue (418 pcm difference) and control rod reactivity worth (1 pcm difference). In terms of radial neutron flux profiles, differences in the inner fuel region were within 5% and 1% for the thermal and fast fluxes respectively. However, in the outer fuel lattice region, differences were considerably higher due to the mismatch between PARCS nodes and heterogeneous fuel pins. Also, PARCS post-processing for intranodal reconstruction proved to be an effective way to observe heterogeneities within nodes, which cannot be otherwise captured by PARCS solution. Some of the modelling challenges were overcome with the use of transport-corrected diffusion coefficients and the implementation of albedo boundary conditions. A parametric analysis reflected the importance of the transport correction of diffusion coefficients for producing good eigenvalues in reactor cores with large neutron leakage.

I. INTRODUCTION

High-confidence computational tools have been developed for full-core 3D reactor core analysis of nuclear power reactors, however the application of these tools for research reactors is not straightforward as there are important differences in geometry, size, operating pressure, coolant flow, and power. In the framework of increasing experimental activities in the CROCUS reactor, it is desired to update the methods for reactor analysis in the quest for improvements in efficiency, safety, and reliability. The Swiss Federal Institute of Technology Lausanne (EPFL) is therefore conducting neutronic modelling and experimental reactor physics activities in the CROCUS reactor.

The goal of the present work is to build a PARCS [1] model of the CROCUS reactor for steady-state and for forthcoming transient calculations. The Serpent Monte Carlo code [2] is used for few-group constant generation. The full-core Serpent model of the reactor is also used as reference for the comparison against PARCS steady-state results. Even though this was attempted in a previous work [3], the present paper implemented important differences in the methodology, namely, the use of the full-scale model of the reactor for few-group constant generation, a transport correction for diffusion coefficients, the use of albedo boundary conditions and form-factors for intranodal reaction rate reconstruction. The present paper describes the methodology used for modelling CROCUS and discusses the challenges encountered during the process.

II. CROCUS REACTOR SPECIFICATIONS

The CROCUS reactor [4] is a two-zone, uranium-fuelled, H₂O-moderated facility operated by the Swiss Federal Institute of Technology Lausanne (EPFL). It can be classified as a zero-power reactor, with a nominal power of 100 W.

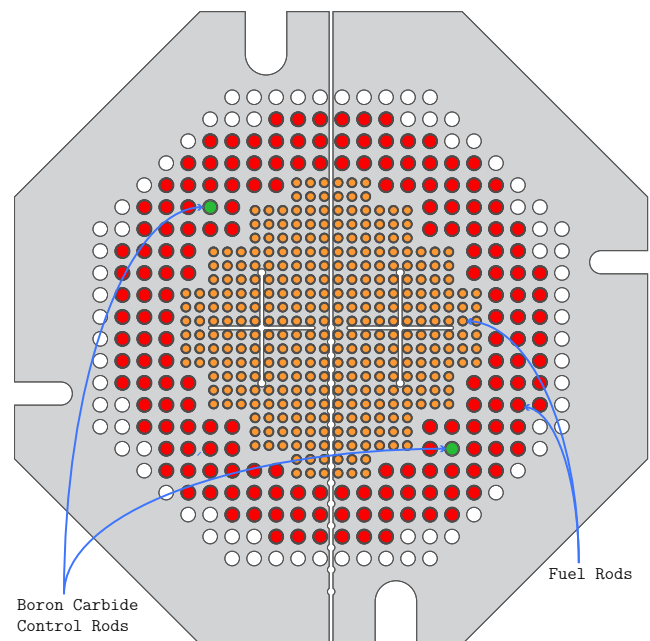


Fig. 1. CROCUS fuel and control rods

The core is approximately cylindrical in shape with a diameter of about 58 cm and a height of 100 cm. The core reactivity is controlled by a variation of the water level with an accuracy of ± 0.1 mm (equivalent to ± 0.4 pcm) and/or by means of two control rods containing naturally enriched boron carbide (B₄C) sintered pellets located symmetrically within the outer core (see Fig. 1).

There are two different kinds of fuel rods within the CROCUS reactor core (see Fig. 1 and 2). The central zone is fuelled with 336 UO₂ fuel rods (1.806 wt%-enriched), which

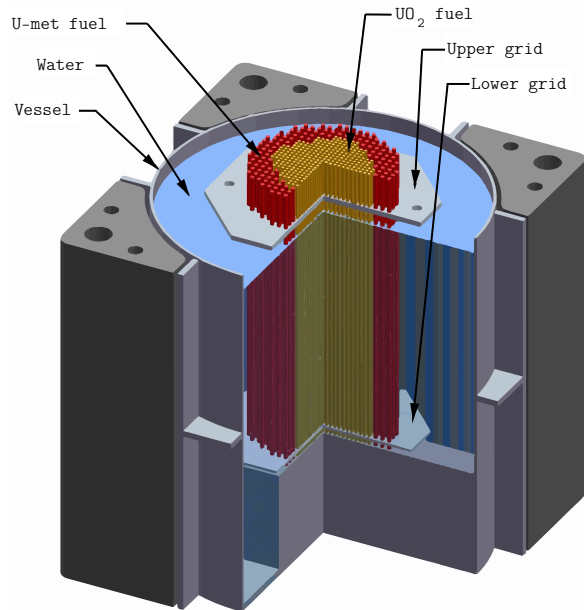


Fig. 2. CROCUS reactor supporting structure and core internals

are thinner rods with a square lattice pitch of 1.837 cm. The peripheral zone is loaded with 176 thicker, U-metal fuel rods (0.947 wt%-enriched) with a pitch of 2.917 cm. All fuel rods have an aluminum cladding and are maintained in a vertical position by the upper grid and lower grid plates spaced 100 cm apart (see Fig. 2). Both grid plates incorporate a cadmium layer with a thickness of 0.50 ± 0.05 mm to limit the axial thermal flux. The active fuel length starts at the top surface of the lower cadmium layer and extends to 100 cm. The core is located in an aluminum water tank whose diameter is 130 cm and thickness is 1.2 cm. Light water (H_2O) is used as moderator and reflector. Because of (1) the different pitches that make the fuel lattices incongruous, (2) the small size of the reactor core, (3) a water-air interface in the active core region and (4) the presence of Cadmium layers in the upper and lower grid plates, modelling the reactor with the PARCS code poses significant challenges. While some of these challenges are related to limitations of diffusion theory (such as the presence of highly absorbing media and the proximity to interfaces), other challenges are linked to software limitations (such as the impossibility of using an unstructured cartesian mesh adaptable to each fuel lattice).

III. PARCS MODELING

Although direct full-core transport calculations (such as DeCART [5], nTRACER [6], and MPACT [7]) are becoming possible with the increase of computational power, they are still under development and more verification and validation (V&V) work needs to be done before they become a standard for reactor analysis. Currently, the full analysis of a nuclear reactor core still relies on the traditional two-step calculation scheme [8], which has been the standard approach for reactor analysis. These steps consists of (1) spatial homogenization and energy group condensation by the lattice code and (2) 3D

full-core calculation using the few-group constants generated in the previous step. A paper by Sanchez [9] provides a good review of modern homogenization techniques.

PARCS is a nodal diffusion code developed by the U.S. Nuclear Regulatory Commission for 3D steady-state and transient analyses [1]. The PARCS code also provides the ability to use the classical Finite Difference Method (FDM) only, which is more suitable for finer mesh structures such as the one in CROCUS. Full-core solutions were provided by the PARCS code with few-group constants generated with the Serpent Monte Carlo code. The Serpent full-core model was also used as reference for comparison against PARCS. This section provides an overview of the development of the PARCS neutronics model.

The CROCUS reactor nodalization is based on nodes equivalent to UO_2 pin cells (inner lattice fuel) in the radial plane (72×72 planar nodes) and 19 axial nodes. The nodalization includes explicit modelling of the radial reflector. Figure 3 shows the radial nodalization for the active core region (reflector nodes are not shown). The colors represent different homogenized cross-section sets. Due to the incongruence between inner and outer fuel lattices pitches (which is reflected in Figure 3) the reactor core cannot be subdivided in simple repeatable subsections (such as fuel assemblies in a PWR). The choice of the PARCS radial nodes to match the inner fuel lattice (i.e. one node per UO_2 fuel pin) was made considering that, from a safety standpoint, accurate power prediction in the inner lattice is of greater importance than for the outer lattice.

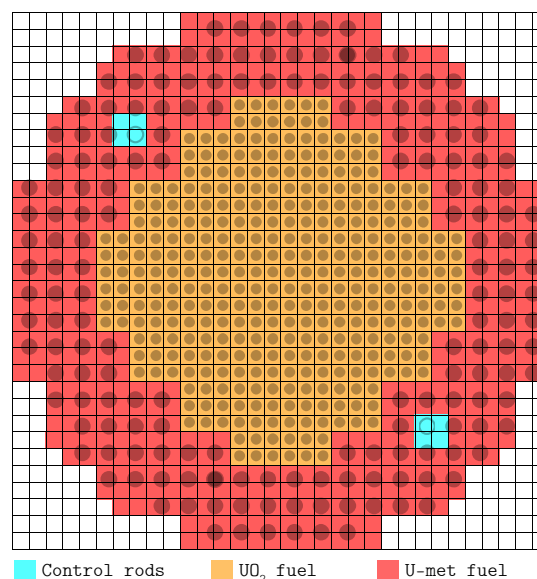


Fig. 3. CROCUS radial plane nodalization

Figure 4 shows the axial nodalization, the different cross-sections sets, and boundary conditions. As mentioned earlier, due to the presence of Cadmium layers in the upper and lower grid plates, albedos (β_G) were used in the axial boundaries for a better prediction of axial leakages.

Control rods were modelled in the radial direction using four nodes for each control rod as shown in Fig. 3.

PARCS solution and form factors were used to reconstruct

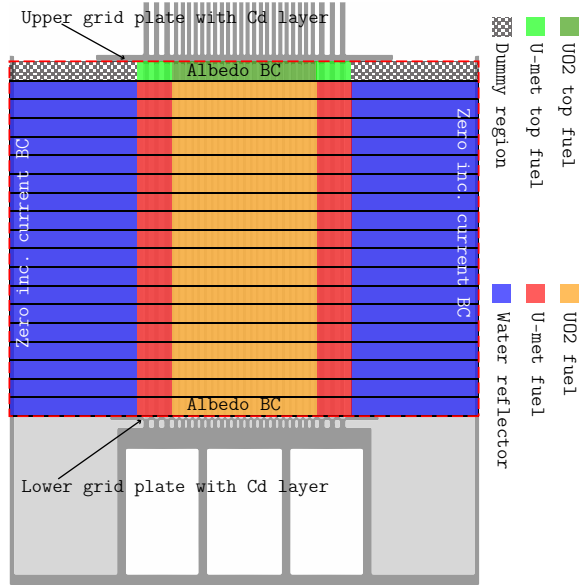


Fig. 4. CROCUS axial nodalization

intranodal fission rate distributions in the radial direction. The form factors are calculated from Serpent fission rate tallies (see the following section) and they are later used to post-process PARCS output data.

PARCS solution was computed using the code version 32m19co with a finite difference (FDM) 2-group diffusion solver.

The Generalised Equivalence Theory [8] establishes that Discontinuity Factors need to be used to preserve the interface fluxes and the net currents from the transport to the diffusion solution. Pin-Cell Discontinuity Factors could have been computed only for the inner lattice fuel but not for the outer lattice fuel due to the mismatch between U-metal pin-cells and PARCS mesh (see Fig. 3). However, no interface discontinuity factors were used since PARCS does not implement them in the FDM solver. The choice of a FDM only solver over the nodal methods available in PARCS is based on the following reasons:

- The node size used for CROCUS modelling is small enough (1.837cm) to converge in space.
- Convergence issues are observed when using nodal methods
- Albedo boundary conditions for rectangular geometries are only available for the FDM solver.
- The use of dummy regions are only available for the FDM solver. Convergence is not reached without the use of dummy regions that are used to replace the air cross-sections (see Fig. 4),

However the use of a FDM solver presents several limitations such as:

- Multi-group diffusion is not supported
- Interface Discontinuity Factors are not supported
- No SP_3 transport solution

IV. FEW-GROUP CONSTANT GENERATION

The few-group constant input for the PARCS code include the following parameters.

- absorption cross-sections ($\Sigma_{a,G}$)
- fission neutron production cross-sections ($\nu\Sigma_{f,G}$)
- fission energy production cross-sections ($\kappa\Sigma_{f,G}$)
- group-to-group scattering cross-sections ($\Sigma_{s,GG'}$)
- fission spectrum (χ_G)
- diffusion coefficients (D_G) or transport cross-sections ($\Sigma_{tr,G}$)

These are the constants needed for forming the multi-group diffusion equations. Also, albedos (β_G), form factors (FF), and detector cross-sections Σ_G^{DET} were input constants for the PARCS code. Even though Discontinuity factors (f_G^s) were not used due to the reason stated earlier, they are also typically used by diffusion codes. All these few-group constants were generated with the Serpent v2.1.27 Monte Carlo code [2]. The use of a Monte Carlo code for lattice physics applications is interesting for reactors like CROCUS, where the geometry cannot be subdivided in smaller repeatable subsections. The Serpent code adds the advantage of being able to extract cross-sections from the full-core geometry rather than from the traditional 2D assemblies with reflective boundary conditions.

Group constants are calculated in Serpent by first homogenizing the geometry using an intermediate (finer) multi-group structure. The data is then collapsed into a coarser energy-group structure with N groups [10]. The Serpent code uses a universe-based geometry model for describing structures. Universes also define the regions where spatial homogenization and energy collapsing take place. By using the full-core Serpent model of the reactor, the whole few-group constants data is produced in multiple universes within a single run.

Seven sets of 2-energy group cross-sections were generated using the full-core model of the reactor. Figures 3 and 4 show in different colors the universes where few-group constants are generated. Note that many of these universes (such as the light blue for control rods and red ones for outer fuel lattice) were deliberately defined to match the PARCS nodes and preserve volumes. The few-group constants were converted into a PARCS-readable format using the GenPMAXS v6.1.3co code [11].

The upper and lower grid plates of the CROCUS reactor are areas of large neutron absorption since they contain a layer of Cadmium. The geometry was axially limited by the grid plates were Albedo boundary conditions ($\beta_G = J_G^-/J_G^+$) were imposed (see Fig. 4).

The JEFF-3.1.1 nuclear data library was used in all Serpent simulations.

1. Form factors for intranodal fission rate modelling

The PARCS code also provides the ability to simulate detector responses, which are computed as

$$R_i = V_i \sum_G \Sigma_G^{DET} \cdot \bar{\phi}_{i,G} \quad (1)$$

Where $\bar{\phi}_i^G$ is the G^{th} group node-average flux in node i and Σ_{DET}^G is the detector cross section which is generated by the Serpent code. Here we are interested to model the fission rate given by a fission chamber that is allowed to move along and across the core and reflector region. Then, these detector cross-sections are computed from Serpent as the ratio of the fission rate to the neutron flux (see Eq. 2).

$$\sum_{f,G}^{DET} = \frac{\int_V \int_{E_i}^{E_{i+1}} \sum_f(r, E) \cdot \phi(r, E) \cdot d^3r \cdot dE}{\int_V \int_{E_i}^{E_{i+1}} \phi(r, E) \cdot d^3r \cdot dE} \quad (2)$$

The fission rate and neutron flux were tallied following the mesh shown in Figure 5. Each node in the mesh has a length (x-direction) equivalent to a PARCS node (1.837 cm) and a width equivalent to the diameter (0.47 cm) of the fission chamber that we are trying to model.

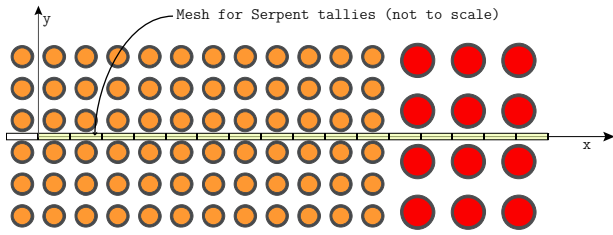


Fig. 5. Serpent mesh for tallying flux and fission rate

PARCS solution and form factors were used to reconstruct the heterogeneous intranodal fission rate distributions in the radial direction. The form factors for node i are calculated from Serpent fission rate $R_{f,i}$ tallies as

$$FF_j = \frac{R_{f,j}}{R_{f,i}} \quad (3)$$

Where the i and j represent the indexes for coarse (equivalent to PARCS solution) and fine (intranodal) fission rate tallies respectively. To tally the intranodal fission rate in Serpent, each node shown in Figure 5 was subdivided in the x-direction into 10 smaller nodes (length of 0.1837 cm), while the width in the y-dimension was kept constant. In that way, the total reaction rates are conserved $\sum R_{f,j} = \sum R_{f,i}$.

The intranodal fission rate is obtained as:

$$R_{f,j}^{\text{intranodal}} = R_{f,i}^{\text{PARCS}} \cdot FF_j \quad (4)$$

Ten form factors per node were generated for a total of 36 nodes which covered the radial direction from the center of the core to the reflector region. The latter implies that 360 intranodal points can be generated for 36 PARCS nodes.

2. Control rods

The control rod cross-sections (see Fig. 3) consist of a main (reference) cross-section set corresponding to the unrodded case, and a branch case corresponding to the rodded

case. The latter was extracted from an additional full Serpent calculation having one control rod fully inserted.

Since the extent of the perturbation caused by the insertion of the control rod goes further away than the four radial nodes used to model each rod, the outer lattice fuel (U-metal fuel) cross-sections need to account for this perturbation as well. Therefore, the cross-sections for the outer lattice fuel are also represented by a main set (in which control rods are withdrawn) and a branch case in which the control rods are fully inserted, which accounts for the perturbation induced by the proximity to the control rods.

3. Light nuclides transport-corrected diffusion coefficient

The original definition of diffusion coefficient implemented in Serpent is that one based on P_1 theory, which assumes that the rate of neutrons from all energies to E (in-scattered neutrons) will approximately balance the rate of neutrons from E to all other energies (out-scattered neutrons). This is the so-called out-scatter approximation for diffusion coefficients [10]. This approximation is accurate enough for large systems where neutron leakage is not very important, however for smaller cores, it produces errors in eigenvalue as large as 1500 pcm (see the Parametric Analysis section).

A correction that accounts for the anisotropic scattering effect for light nuclides [12] (such as Hydrogen for LWR) was recently implemented in the latest version of the Serpent code (v2.1.27).

The correction method uses a user-defined energy-dependent transport correction curve adapted to the light nuclide responsible for the scattering anisotropy. The correction curve $f(E)$ represents the ratio of transport cross section to total cross section of this isotope.

$$f(E) = \frac{\Sigma_{tr}(E)}{\Sigma_{tot}(E)} \quad (5)$$

It is assumed that in a Light Water Reactor most of the anisotropic scattering will occur in hydrogen bound to water. In such case, the correction is made for the ^1H isotope, and the correction curve $f(E)$ is generated from a slab of pure hydrogen.

Having the pre-computed correction curve for hydrogen $f_{\text{H}}(E)$, the transport-corrected (TRC) hydrogen transport cross-section is computed by the lattice code as,

$$\Sigma_{tr,H}^{\text{TRC}}(E) = \Sigma_{tot,H}(E) \cdot f_{\text{H}}(E) \quad (6)$$

Finally, the transport-corrected (TRC) hydrogen transport cross section is added with the transport cross section for all other isotopes after removing the non-corrected hydrogen transport cross section.

$$\Sigma_{tr,\text{all}}^{\text{TRC}}(E) = \Sigma_{tr,\text{all}}(E) - \Sigma_{tr,H}(E) + \Sigma_{tr,H}^{\text{TRC}}(E) \quad (7)$$

Then, the energy variable can be collapsed and these transport cross sections are used for calculating diffusion coefficients as $D = 1/3\Sigma_{tr}$.

A detailed description of this correction can be found in paper by Herman [12].

V. CODE-TO-CODE COMPARISON RESULTS

PARCS code solution was compared against that one of Serpent for integral parameters such as eigenvalue and integral control rod reactivity worth, and for local information such as neutron fluxes and ^{235}U fission rate profiles. Given the ability of Monte Carlo codes to perform full-core steady-state neutronics calculations with a high level of detail, the Serpent solution was used as reference for the comparison. High number of neutron histories (10^4 cycles of 10^6 neutrons each) were used in Serpent to reduce the eigenvalue statistical uncertainty to one pcm, and below 0.5% for fission rates and neutron fluxes.

	k_{eff}	$\frac{\Delta k}{k}$ [pcm]
Serpent (reference)	1.00166 ± 0.00001	
PARCS - 2G diffusion	0.99747	-418

TABLE I. Eigenvalue comparison

Table I shows the eigenvalues comparison between Serpent and PARCS. Considering the limits of diffusion theory and the characteristics of the CROCUS reactor earlier presented, good agreement was achieved with a difference of -418 pcm with respect to Serpent solution. The effect of core size in the prediction of eigenvalue is reflected in the diffusion coefficient study presented in the Parametric Analysis section.

A mesh refinement was performed over the PARCS solution to check for spatial convergence. The results were computed using a 2-group FDM diffusion solver and are shown in Table II.

mesh size [cm]		run time	k_{eff}	$\frac{\Delta k}{k}$ [pcm]
x, y	z	[MM:SS]		
1.8370	5.2622	00:02	0.997476	-
0.9185	2.6311	00:44	0.997426	-5.0
0.4592	1.3155	10:20	0.997399	-7.7

TABLE II. PARCS mesh refinement results

The integral control rod reactivity worth for one rod are also compared with Serpent in Table III, and the agreement between codes is excellent. This high level of agreement was achieved after implementing a branch case for "rodded case" in outer fuel lattice cross-section set as mentioned earlier in the previous section.

	Control rod reactivity worth [pcm]
Serpent (reference)	170 ± 1
PARCS - 2G diffusion	171

TABLE III. Control rod reactivity worth comparison

Detectors were used to compute fission rate distributions in the PARCS code at a coarse level (node size = 1.837 cm). Cross-section data for these detectors were generated by the Serpent code. Figure 6 shows the comparison of relative ^{235}U fission rate distributions between the two codes. Intranodal reconstruction was used to increase the spatial resolution to

be able to predict the dips and bumps in the profiles. This information cannot be captured by the PARCS homogeneous solution given the size of the nodes. The relative difference shown in the figure was calculated between the "PARCS intranodal" fission rate reconstruction and the Serpent reference. The PARCS nodal solution (red circles) was added to the figure to highlight the difference between nodal and intranodal profiles. The profiles were taken from an axial slice in the mid-plane of the core. In the radial direction they begin at the center of the core ($r = 0$) and finish in the reflector region. The profiles are normalised with respect to the integral under the curve. The agreement between codes for radial fission rate profiles is very good considering the limitations of the code and diffusion theory. As expected, larger differences were found in the UO_2/U -metal fuel lattices interface ($r = 20.2$ cm), at the outer fuel lattice where PARCS nodes and explicit fuel pins are incongruent, and near the core periphery ($r = 29.17$ cm).

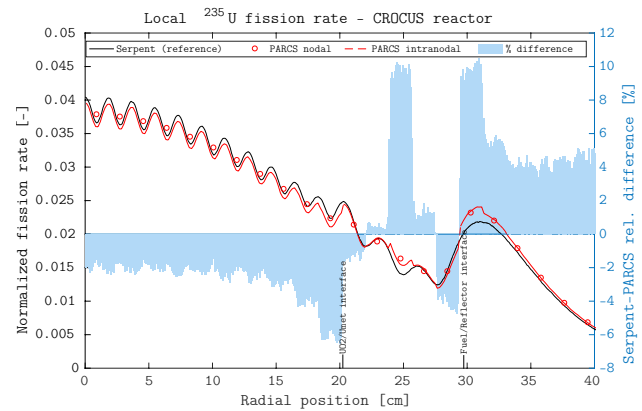


Fig. 6. CROCUS radial ^{235}U fission rate profile

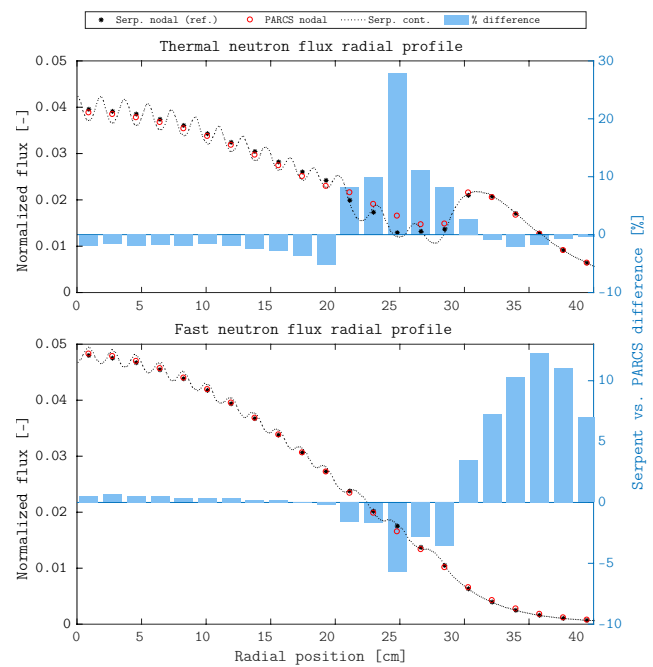


Fig. 7. CROCUS radial neutron flux profiles

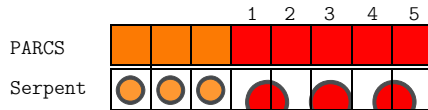


Fig. 8. Homogeneous (PARCS) and heterogeneous (Serpent) modelling of outer lattice fuel nodes

Figure 7 shows the radial thermal and fast neutron flux profiles predicted by the PARCS and Serpent codes. For the “Serpent nodal” profile, the neutron fluxes were tallied using a mesh matching the PARCS nodes size (1.837 cm x 1.837 cm x 5.26 cm). The “Serpent continuous” profile uses a finer mesh in the radial direction. These profiles were taken from one axial plane in the center of the core. The profiles were also normalized with respect to the integral under each curve. The right axis shows the relative differences between PARCS and “Serpent nodal” fluxes. Differences in the inner fuel region ($r < 20$ cm) are within 5% and 1% for the thermal and fast fluxes respectively. However, in the outer fuel lattice (where PARCS nodes and the heterogeneous fuel pins are incongruent) and core periphery, differences are considerably higher. These differences can be explained by observing Figure 8. While each PARCS node of the outer lattice has the same fuel/moderator ratio (because it is an homogeneous mixture), in the Serpent model the fuel/moderator ratio will vary from node to node. Figure 8 shows that node 3 of the Serpent model has a larger fuel/moderator ratio as compared to the neighboring nodes; therefore the heterogeneous Serpent model is expected to reflect, at that point, a dip in the thermal flux and a bump in the fast flux, which is consistent with the results presented in Figure 7 (see results nearby $r = 25.7$ cm).

Comparison of the axial neutron flux profiles is shown in the albedos study presented in the parametric analysis section.

VI. PARAMETRIC ANALYSIS

1. Transport correction of diffusion coefficients

As mentioned earlier, in reactors with large neutron leakage like CROCUS, diffusion coefficients play a big role for producing good eigenvalues.

The light nuclides transport correction of diffusion coefficients (TRC) has been compared against the traditional out-scatter approximation for diffusion coefficients.

	k_{eff}	$\frac{\Delta k}{k}$ [pcm]
Serpent (reference)	1.00166 ± 0.00001	
PARCS - no correction	0.98543	-1620
PARCS - with TRC	0.99747	-418

TABLE IV. Impact of transport-corrected diffusion coefficient on CROCUS k_{eff}

Table V shows that a significant improvement in CROCUS eigenvalue (around 1200 pcm) was achieved with the use of the transport correction. The last column shows the difference with respect to Serpent. Figure 9 shows that the thermal flux profiles are also improved after the transport correction, in particular in the center of the core.

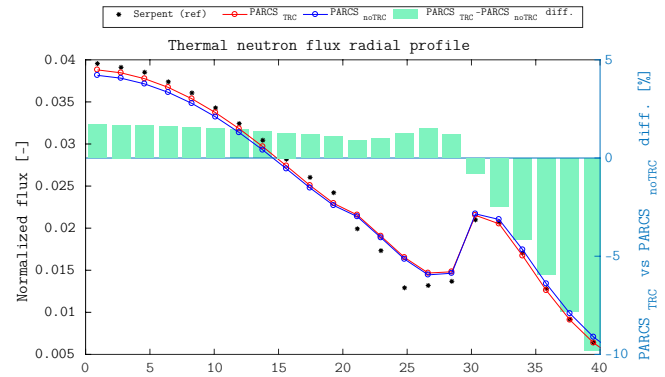


Fig. 9. Impact of transport-corrected diffusion coefficient on thermal neutron flux radial profile

Simpler models were built to further study the effect of the transport correction in eigenvalue prediction. The objectives of the study are:

- To verify that the improvements shown in Table V and Figure 9 are not due to compensation of errors.
- To determine if the impact of the transport correction is more significant for smaller cores with large neutron leakage than for cores with more limited leakage.

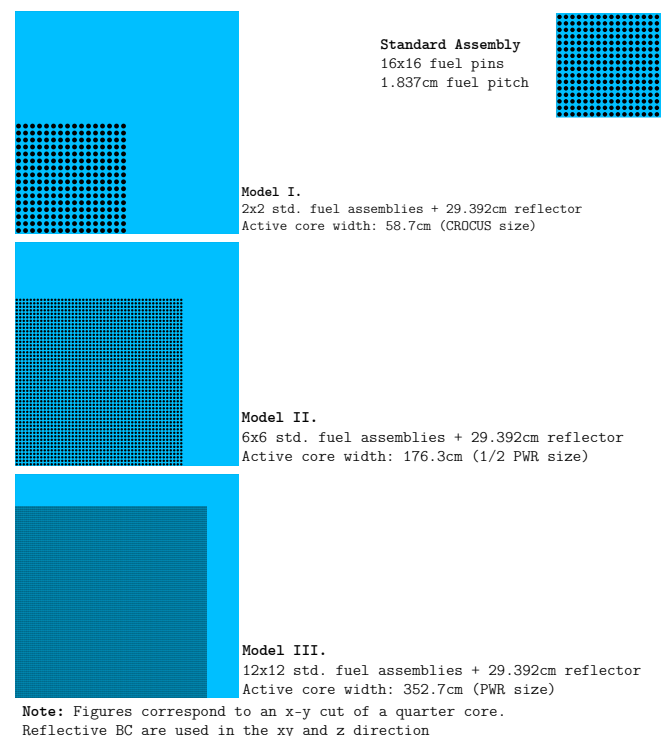


Fig. 10. Models used for the study of transport-corrected diffusion coefficients.

Figure 10 shows the three models that were built based on a standard assembly containing 16x16 fuel pins. The assembly fuel pitch is 1.837 cm loaded with U-metal fuel and light

water moderated. The same reflector thickness (29.39 cm) was used for all models and reflective boundary conditions were imposed in all three directions. Two sets of few-group constants (for fuel and reflector) were generated by Serpent using quarter-core symmetry as show in Figure 10. Two-group diffusion solutions were computed using the PARCS code.

	k_{eff}	$\frac{\Delta k}{k}$ [pcm]
Model I (core width: 58.7cm)		
Serpent (reference)	0.95574 ± 2 pcm	
PARCS - no correction	0.94556	-1065
PARCS - with TRC	0.95359	-225
Model II (core width: 176.3cm)		
Serpent (reference)	1.05662 ± 1 pcm	
PARCS - no correction	1.05548	-108
PARCS - with TRC	1.0566	-2
Model III (core width: 352.7cm)		
Serpent (reference)	1.07040 ± 1 pcm	
PARCS - no correction	1.07017	-21
PARCS - with TRC	1.07046	+6

TABLE V. Impact of transport-corrected diffusion coefficient on k_{eff} for various core sizes.

Table V shows the Serpent and PARCS eigenvalue results for all three models. The effect of the transport-corrected diffusion coefficient becomes clear for Model I, where the improvement in k_{eff} with respect to the Serpent reference is of 840 pcm. For Model III (PWR-equivalent size), the transport correction seems to have a minor effect on eigenvalue, however as the core size decreases (Model II and I), this correction has a larger impact potentially due to an increase in the neutron leakage from fuel to reflector zone.

2. Energy-group structure

The energy group structure is another parameter that might have an impact on eigenvalue and power distributions. Since multigroup diffusion is not supported by the PARCS' FDM solver (which was used in the code-to-code comparison), it was required to simplify the CROUCS model to be able to run it with the multi-group nodal expansion method (NEMMG) solver in PARCS. The following models changes were applied to the original CROUCS model presented in the results section:

- The dummy regions in the top of the fuel were replaced by water.
- The albedo boundary conditions, which were set at the axial boundaries, were replaced by void (zero incoming current) boundary conditions. The axial boundaries remained limited to the grid plates as it was done with the original CROUCS model.

The NEMMG solver was used to compute diffusion solutions for 2, 4, 8, 16, and 40 energy groups. A 70-group structure was also tested, however the solution did not converge.

	k_{eff}	$\frac{\Delta k}{k}$ [pcm]
Serpent* (reference)	1.00200 ± 3 pcm	
PARCS - 2G diffusion	0.99535	-664
PARCS - 4G diffusion	0.99362	-836
PARCS - 8G diffusion	0.99247	-951
PARCS - 16G diffusion	0.99241	-957
PARCS - 40G diffusion	0.99262	-936

TABLE VI. Impact of energy-group structure on k_{eff} . *Note: Serpent and PARCS results correspond to a simplified model (not for CROUCS).

The energy-group structures were taken from CASMO-4 [13]. Table VI shows the eigenvalue predictions and their difference with respect to the Serpent reference. Serpent and PARCS results correspond to a simplified model as described above and not for CROUCS. These results suggest that, for these type of reactors, the eigenvalue tends to be more under-predicted after refining the energy-group structure. However the change on k_{eff} with respect to the two-group solution is limited to around 300 pcm.

The effect of refining the energy-group structure was also studied in terms of radial power distribution. Figure 11 shows the radial power distribution difference with respect to the two-group solution. Differences are small and contained within 0.4% and 0.8% in the inner lattice fuel and outer lattice fuel regions respectively, which suggests that the refinement of the energy-group structure has a minimal effect on power prediction in a CROUCS-comparable problem.

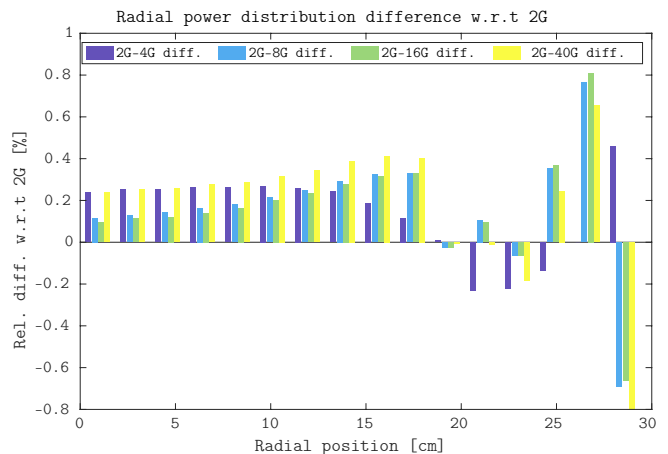


Fig. 11. Multigroup diffusion - Radial power distribution difference with respect to two-group structure.

3. Reduced geometry with albedo BC vs. full geometry with void BC

Albedo boundary conditions were imposed to (1) avoid modelling the Cadmium layers (strong neutron absorbers) using diffusion theory, (2) to adjust the neutron leakage in the grid plates where Cd is present, and (3) to reduce the geometry to the active core region for a tighter and faster problem convergence.

	k_{eff}	$\frac{\Delta k}{k}$ [pcm]
Serpent (reference)	1.00166 ± 1 pcm	
PARCS - albedo BC ¹	0.99747	-418
PARCS - void BC ²	0.99660	-505

TABLE VII. Impact of albedo boundary conditions on k_{eff} . ¹Albedo BC: Reduced geometry. ²Void BC: Full geometry.

The solution with albedo boundary conditions was compared to the full geometry solution (with void BC) that models the regions in the top and bottom of the active core (recall Fig. 4). Table VII shows the eigenvalue comparison of these two models against the Serpent model. The eigenvalue is better predicted with the use of albedos BC. However, in terms of neutron flux axial profile, the solution with albedo BC shows lower performance than the full core solution with void BC in the bottom region of the core. This can be observed in Figure 12. This unexpected result might be attributed to compensation of errors.

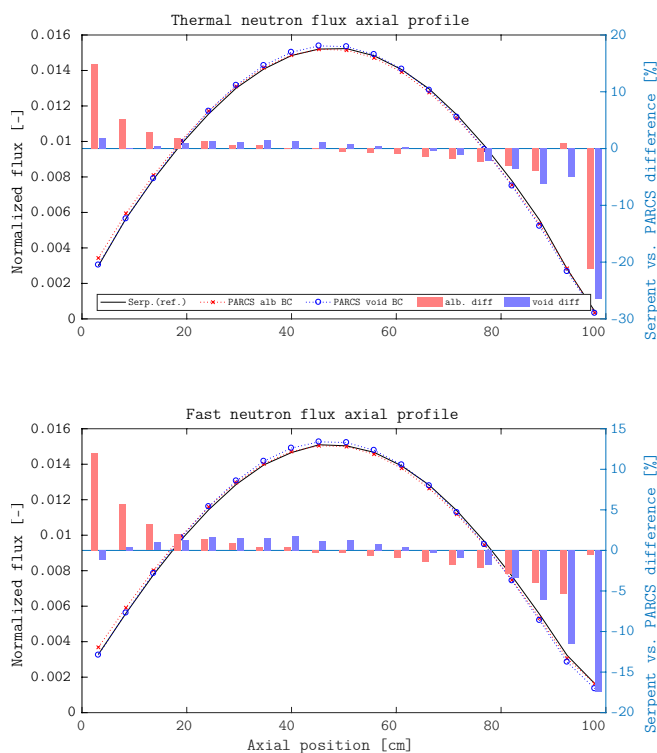


Fig. 12. CROCUS axial neutron flux profiles. Albedo BC (reduced geomtry) vs. Void BC (full geometry).

VII. CONCLUSIONS

The challenges of modelling the CROCUS with the PARCS code are related to limitations of diffusion theory -such as the presence of highly absorbing media and the proximity to interfaces-, but they are also linked to software limitations -such as the impossibility of using an unstructured cartesian mesh adaptable to each fuel lattice-. Efforts to cope with some of these limitations include the use of the Serpent code

for generation of few-group constants, the use of transport-corrected diffusion coefficients, the implementation of albedo boundary conditions, and data post-processing for intranodal reconstruction.

The use of Monte Carlo codes such as Serpent for producing few-group constants for reactor core simulators results advantageous when dealing with irregular geometries and relatively small geometries, where the computational cost remains acceptable. The full-scale heterogeneous solution from the Monte Carlo code can be used not only to extract few group constants from the actual infinite flux and spectrum, but also as reference for the verification of steady-state solutions.

Comparison between Serpent and PARCS solutions for the CROCUS model was successful, achieving good level of agreement for eigenvalue (418 pcm difference) and control rod reactivity worth (1 pcm difference). In terms of radial fission rate and neutron flux profiles, the most important differences were found at the outer fuel lattice region -where PARCS nodes and fuel pins are incongruent- and in the reflector region. PARCS' output post-processing for intranodal reconstruction proves to be an effective way to observe heterogeneities within nodes, which cannot be otherwise captured by PARCS solution.

The parametric analysis carried out in this work reflects the importance of the transport correction of diffusion coefficients for producing good eigenvalues. For the CROCUS reactor, this improvement is of 1200 pcm, however for cores with more moderate neutron leakages, the improvement on k_{eff} is less important. This transport correction has also a positive impact on the thermal neutron flux distribution, in particular in the center of the core.

Refining the energy-group structure seems to have a minor but negative impact on k_{eff} . The impact on radial power distribution is also minor.

The implementation of albedo boundary conditions in the axial direction is successful in reducing computational resources, as the geometry can be reduced to the active core region. Albedos are also responsible for a modest improvement in k_{eff} of around 90 pcm. However, in terms of axial neutron profiles, the solution with albedo boundary conditions shows lower performance in the bottom region of the core than the full core solution with void boundary conditions. This result might be attributed to compensation of errors.

VIII. FUTURE WORK

Static and transient experiments have been carried out in the CROCUS reactor. While the static experiments have been compared against the Serpent code in a previous work [14], the comparison of these experiments against PARCS solution is being prepared for the publication of a journal paper.

PARCS simulations of the transient experiments are in progress. Results of these simulations will also be published.

REFERENCES

1. T. J. DOWNAR, D. A. BARBER, R. M. MILLER, C.-H. LEE, T. KOZLOWSKI, D. LEE, Y. XU, J. GAN, H. G. JOO, J. Y. CHO, ET AL., "PARCS: Purdue advanced

- reactor core simulator,” in “Proc. Int. Conf. on the New Frontiers of Nuclear Technology: Reactor Physics, Safety and High-Performance Computing,” (2002), pp. 7–10.
2. J. LEPPÄNEN, “SERPENT Monte Carlo reactor physics code,” (2010).
 3. A. RAIS, D. SIEFMAN, G. GIRARDIN, M. HURSIN, and A. PAUTZ, “Methods and Models for the Coupled Neutronics and Thermal-Hydraulics Analysis of the CROCUS Reactor at EFPL,” *Science and Technology of Nuclear Installations*, **2015** (2015).
 4. R. FRÜH, “Réacteur CROCUS, Complément au rapport de sécurité: Réactivité et paramètres cinétiques,” (1993).
 5. H. G. JOO, J. Y. CHO, K. S. KIM, C. C. LEE, and S. Q. ZEE, “Methods and performance of a three-dimensional whole-core transport code DeCART,” (2004).
 6. Y. JUNG, “nTRACER v1. 0 Methodology Manual,” *SNURPL-CM001 (10)*, Seoul National University Reactor Physics Laboratory, Seoul, Republic of Korea (2010).
 7. B. KOCHUNAS, B. COLLINS, D. JABAAY, T. DOWNAR, and W. MARTIN, “Overview of development and design of MPACT: Michigan parallel characteristics transport code,” Tech. rep., American Nuclear Society, 555 North Kensington Avenue, La Grange Park, IL 60526 (United States) (2013).
 8. K. S. SMITH, *Spatial homogenization methods for light water reactor analysis*, Ph.D. thesis, Massachusetts Institute of Technology (1980).
 9. R. SANCHEZ, “Assembly homogenization techniques for core calculations,” *Progress in Nuclear Energy*, **51**, 1, 14–31 (2009).
 10. J. LEPPÄNEN, M. PUSA, and E. FRIDMAN, “Overview of methodology for spatial homogenization in the Serpent 2 Monte Carlo code,” *Annals of Nuclear Energy*, **96**, 126–136 (2016).
 11. A. WARD, Y. XU, and T. DOWNAR, “GenPMAXS,” *University of Michigan* (2013).
 12. B. R. HERMAN, B. FORGET, K. SMITH, and B. N. AVILES, “Improved diffusion coefficients generated from Monte Carlo codes,” Tech. rep., American Nuclear Society, 555 North Kensington Avenue, La Grange Park, IL 60526 (United States) (2013).
 13. M. EDENIUS, K. EKBERG, B. H. FORSSÉN, and D. KNOTT, “CASMO-4, A Fuel Assembly Burnup Program, User’s Manual,” *StudsvikOSOA-9501*, Studsvik of America, Inc (1995).
 14. P. G. P. A. RAIS A, HURSIN M, “Experimental Validation of Control Rod Reactivity Worth and Fission Rate Distributions for the CROCUS Reactor,” *PHYSOR* (2016).